Second Order Nonlinear Electromagnetic Interactions in Nanoscale Ferroelectric Thin Films on Metal Substrates

Jeffrey F. Webb *

* *Swinburne University of Technology Sarawak Campus, 93576 Kuching, Sarawak, Malaysia (e-mail: jeffwebb@physics.org).*

Abstract: The Landau-Ginzburg phenomenological theory of ferroelectrics together with Landau-Khalatnikov equations of motion are applied to the problem of studying the interaction of electromagnetic radiation and a ferroelectric nanoscale thin film on a metal substrate. A cornerstone of the analysis is the minimization of a Gibb's free energy functional that takes into account the free energy cost of the boundaries of the thin film via a gradient term that is non zero when the polarization in the film varies. The minimization procedure involves the calculus of variations and leads to an Euler-Lagrange equation that can be solved to find the equilibrium polarization in the film. With this found the nonlinear dynamical equations that describe the response to an incident electromagnetic field are solved by using a perturbation expansion of the polarization expanded about the equilibrium polarization in powers of the incident electric field. The solution method is similar to the Frobenius method. We pick out a second order nonlinear effect from the expansion for second harmonic generation; calculate a reflection coefficient for the harmonic generation term and investigate how the finite thickness of the film influences the reflection coefficient. This paves the way for experimental studies using far-infrared or terahertz reflection measurements (the ferroelectric film is resonant in the far infrared and terahertz ranges) that may help to elucidate the nature of the nonlinear interactions.

Keywords: Ferroelectric, film, nonlinear, electromagnetic, size effects.

1. INTRODUCTION

In this paper the Landau-Devonshire phenomenological theory of ferroelectrics is used together with the Maxwell wave equation to calculate the second-harmonic generation (SHG) component of the nonlinear interaction of a ferroelectric-thin film with incident electromagnetic radiation. However it is the electric field part of the wave that is responsible for most the interaction since the magnetic interaction is small enough to neglect. So in what follows are main concern is with the electric field and the way in which it interacts on the macroscopic scale with the ferroelectric film whose presence on this scale is introduced into the Maxwell equations through the concept of polarization, which is a macroscopic quantity defined defined on that scale as dipole moment per unit volume. The work here is particularly concerned with finding the reflection coefficient associated with the SHG field generated in the film.

There are several motivations for this work. One is that using SHG has been found to be a sensitive optical technique for characterizing the domain structure of ferroelectric thin films. See Bottomley et al. (2001), Gopalan and Raj (1996), Barad et al. (2001), and Mishina et al. (2003). Another is that there is a strong interest in ferroelectric thin films due to applications in ferroelectric random access memories (FERAMs) (Scott (1998), Auciello et al. (1998) and Scott (1992)), and it is important to study how the film surfaces affect the polarization, especially at the nanoscale.

The approach taken in this paper is to calculate the SHG interaction with a ferroelectric film using a phenomenological theory based on Landau-Devonshire theory (discussed by Lines and Glass (1977), for example) which models the overall ferroelectric properties including the static equilibrium polarization and Landau-Khalatnikov equations to describe the dynamic response of the polarization to an external electric field. Other work on ferroelectric films using a similar theoretical approach has been done by Stamps and Tilley (1999), Chew et al. (1999), Tan et al. (2000), Chew et al. (2001), Ong et al. (2001), Murgan et al. (2004) and Webb (2006).

We will consider a nanoscale ferroelectric film, above which is air and the bottom surface of the film is in contact with a metal substrate.The coordinate system will be chosen such that the air-film interface is at $z = 0$, and the film-metal interface is at $z = -L$, where L is the film thickness. The speed of propagation in air will be taken to be equal to the speed of light in vacuum at all frequencies. It is of interest to consider a conducting substrate because in applications such as FERAMs electrical contacts with the film need to be made.

2. FORMALISM

The Landau-Devonshire theory is based on the Gibbs free energy thermodynamic potential expanded in powers of the polarization P (see Lines and Glass (1977)). For a ferroelectric film of thickness L in which the polarization is allowed to vary with distance into the film such that $P = P(z)$, this takes the form of a functional given by

$$F/S = \int_{-L}^{0} f(P, dP/dz)\, dz + (D/2)[P^2(-L)/\delta_1 + P^2(0)/\delta_2], \tag{1}$$

where

$$f(P, dP/dz) = (1/2)AP^2 + (1/4)BP^4 + (1/6)CP^6 + (D/2)(dP/dz)^2 - \mathbf{E}\cdot\mathbf{P} \tag{2}$$

and

$$A = a(T - T_0). \tag{3}$$

In the ferroelectric phase there is a spontaneous polarization that exists when the applied field $\mathbf{E}$ is zero. The spontaneous polarization depends on temperature. Here we consider the case in which the transition from the ferroelectric phase to the paraelectric phase (no spontaneous polarization) is second order. In this case the transition occurs at a single temperature, $T_0 = T_C$, where T_C is the Curie temperature, which is the temperature at which the second-order phase transition occurs; B is a constant greater than zero and $C = 0$. For first-order transitions, not considered here, $B < 0$ and $C > 0$. The inclusion of the C terms creates a discontinuous jump when the phase changes from ferroelectric to paraelectric, consistent with what is observed experimentally for first order phase transitions. Second order transitions do not exhibit such a discontinuity; instead the polarization approaches zero continuously as $T_C \to 0$. See Strukov and Lenanyuk (1998) for a more thorough discussion. In both cases a is a positive constant (the inverse of the Curie constant). The temperature variation modeled by (3) is derived by considering the temperature function as a Taylor series to first order in T. However this approximation may break down at temperatures very far from, or close to the transition temperature. The gradient term in $(D/2)(dP/dz)^2$ in f takes into account the free-energy cost of spatial variations in the polarization which are important near the surfaces (in the bulk the spontaneous polarization is constant), and the terms after the integral in (1) are surface energy terms that arise from integrating over the film surfaces. The parameters δ_1 and δ_2, as discussed by Webb (2006), are extrapolation lengths used to set boundary conditions for the spontaneous polarization at the surfaces. If the media above and below the film are the same then $\delta_1 = \delta_2$. These are size-effect parameters introduced due to the need for having boundary conditions. And they, along with the constants B and C are phenomenological parameters; they are not derived from first principles, but rather they are considered as parameters who's values could be found from experimental data. An interesting discussion of related size-effects is given by Tagantsev et al. (2008)

The key idea for finding spontaneous polarization, denoted by P_0, is that it is the function (of z) that minimizes the free energy in (1) under the condition $\mathbf{E} = 0$. Finding P_0 is thus a calculus of variations problem that leads to the Euler-Lagrange equation (for our case in which $C = 0$):

$$D\frac{d^2P_0}{dz^2} - AP_0 - BP_0^3 = 0 \tag{4}$$

with boundary conditions

$$dP_0/dz - P/\delta_1 = 0 \quad \text{at } z = -L \tag{5}$$

and

$$dP_0/dz - P/\delta_2 = 0 \quad \text{at } z = 0. \tag{6}$$

An analytical solution to this problem can be found that gives $P_0(z)$ in terms of elliptic functions (see Tilley and Zeks (1984), Ong et al. (2001) and Webb (2006) for details). It can be seen from (5) and (6) that an extrapolation length with a negative value implies that $P_0(z)$ increases as the corresponding surface is approached; conversely a positive value causes a decrease in $P_0(z)$.

Dynamic coupling to the electromagnetic field (via $\mathbf{E}$) is described by means of the Landau-Khalatnikov (LK) equations of motion,

$$m\frac{\partial^2\mathbf{P}}{\partial t^2} + \gamma\frac{\partial\mathbf{P}}{\partial t} = -\boldsymbol{\nabla}_\delta F = -\left(D\frac{\partial^2\mathbf{P}}{\partial z^2} - A\mathbf{P} - B\mathbf{P}^3\right) + \mathbf{E}, \tag{7}$$

in which m and γ are, respectively, mass and damping parameters, and $\boldsymbol{\nabla}_\delta = \hat{\mathbf{x}}(\delta/\delta P_x) + \hat{\mathbf{y}}(\delta/\delta P_y) + \hat{\mathbf{z}}(\delta/\delta P_z)$, which involves variational derivatives, and we introduce the term variational gradient-operator for it, noting that $\hat{\mathbf{x}}$, $\hat{\mathbf{y}}$ and $\hat{\mathbf{z}}$ are unit vectors along positive x, y and z, respectively. Note that this equation is analogous to the equation of motion for a damped mass-spring system undergoing forced vibrations. However here it is the electric field $\mathbf{E}$ that provides the driving impetus for $\mathbf{P}$ rather than a force explicitly. Also note that the potential term $\boldsymbol{\nabla}_\delta F|_{\mathbf{E}=0}$ is analogous to a nonlinear force-field (through the nonlinear P terms in (2)) rather than the linear Hook's law force commonly employed to model a spring-mass system. The variational derivatives are given by

$$\frac{\delta F}{\delta P_x} = \left(A + 3BP_0^2\right)Q_x + B\left(2P_0Q_x^2 + P_0Q^2 + Q^2Q_x\right) - D\frac{\partial^2 Q_x}{\partial z^2} - E_x \tag{8}$$

and

$$\frac{\delta F}{\delta P_\alpha} = \left(A + BP_0^2\right)Q_\alpha + B\left(2P_0Q_xQ_\alpha + Q^2Q_\alpha\right) - D\frac{\partial^2 Q_\alpha}{\partial z^2} - E_\alpha, \quad \alpha = y \text{ or } z, \tag{9}$$

where $Q^2 = Q_x^2 + Q_y^2 + Q_z^2$, and $\mathbf{P}$ has been written as a sum of static and dynamic parts, $P_x = P_0(z) + Q_x$, $P_y = Q_y$, and $P_z = Q_z$. In doing this we have orientated $\mathbf{P}_0(z)$ so that it is parallel to the film surfaces in the direction of positive x. This is done to simplify the problem so that we can focus on the essentials of SHG in subsequent calculations. It should be noted that if $\mathbf{P}_0(z)$ had a z component, depolarization effects would need to be taken in to account in the free energy, and a theory for doing this has been presented by Tilley (1993). The in-plane orientation avoids this complication. The LK equations in (7) are appropriate for displacive ferroelectrics that are typically used to fabricate thin films (see Lines and Glass (1977) and Scott (1998) for more on this), with $BaTiO_4$ being a common example. Displacive ferroelectrics have a spontaneous polarization due to a lattice displacement and the dynamic response is due lattice vibrations.

The LK equations describe the dynamic response of the polarization to the applied field. Also the polarization and electric field must satisfy the inhomogeneous wave equation derived from Maxwell's equations. This wave equation is:

$$\frac{\partial^2 E_\alpha}{\partial x^2} - \frac{\epsilon_\infty}{c^2}\frac{\partial^2 E_\alpha}{\partial t^2} = \frac{1}{c^2\epsilon_0}\frac{\partial Q_\alpha}{\partial t^2}, \quad \alpha = x, y, \text{ or } z. \tag{10}$$

Here, c is the speed of light in vacuum, ϵ_0 is the permittivity of free space, and ϵ_∞ is the contribution of high frequency resonances to the dielectric response. The reason for including it is as follows. Displacive ferroelectrics, in which it is the lattice vibrations that respond to the electric field, are resonant in the far infrared and terahertz wave regions of the electromagnetic spectrum and that is where the dielectric response calculated from the theory here will have resonances. There are higher frequency

resonances that are far from this and involve the response of the electrons to the electric field. Since these resonances are far from the ferroelectric ones of interest here they can be accounted for by the constant ϵ_∞.

Solving equations (8) to (10) for a given driving field $\mathbf{E}$ will give the relationship between $\mathbf{P}$ and $\mathbf{E}$, and the way that the resulting electromagnetic waves propagate above and in the film can be found explicitly. However it is also necessary to postulate a constitutive relationship between $\mathbf{P}$ and in the perturbation-expansion approach (see Butcher and Cotter (1990)) that will be used here it takes the form

$$\mathbf{Q} = \mathbf{P} - \mathbf{P}_0 = \mathbf{Q}^{(1)}(t) + \mathbf{Q}^{(2)}(t) + \ldots, \tag{11}$$

where $\mathbf{Q}^{(1)}(t)$ is the linear with respect to the input field, $\mathbf{Q}^{(2)}(t)$ is quadratic, and so on for higher order terms. For SHG it is not necessary go beyond the quadratic term, however. The way in which he the electric field enters is through time integrals and response function tensors as follows:

$$\mathbf{Q}^{(1)}(t) = \epsilon_0 \int_{-\infty}^{+\infty} d\tau\, \mathbf{R}^{(1)}(\tau) \cdot \mathbf{E}(t-\tau) \tag{12}$$

and

$$\mathbf{Q}^{(2)}(t) = \epsilon_0 \int_{-\infty}^{+\infty} d\tau_1 \int_{-\infty}^{+\infty} d\tau_2\, \mathbf{R}^{(2)}(\tau_1, \tau_1') : \mathbf{E}(t-\tau_1)\mathbf{E}(t-\tau_2). \tag{13}$$

The time integrals appear because in general the response is not instantaneous; at any given time it also depends on the field at earlier times—there is temporal dispersion. Analogous to this there is spatial dispersion which would require integrals over space. However this is often negligible and is not a strong influence on the thin film calculations that we are considering. For an in-depth discussion see Mills (1991).

Of particular interest is the reflection coefficient since this can be measured using far infrared or terahertz spectroscopy. In such experiments it is convenient to use a single frequency input field whose frequency can be changed and the corresponding variations in reflectivity can be measured. Therefore it is useful to consider a single frequency sinusoidal form for $\mathbf{E}$, which is what will be done in the calculations that follow.

3. CALCULATION OF THE REFLECTION COEFFICIENT FOR SHG

3.1 General Considerations and Simplifications

The incident field is taken to be a plane wave of frequency ω and wave number above the film has a magnitude $q_0 = \omega/c$, since the region above the film behaves like a vacuum in which all frequencies propagate at c. We only consider normal incidence and note that the field is traveling in the negative z direction in the coordinate system used here in which the top of the film is in the plane $z = 0$, the bottom in the plane $z = -L$. Therefore $\mathbf{q}_0 = q_0(-\hat{\mathbf{z}})$ and the incident the incident field can be represented by

$$(1/2)\mathbf{E}_0 e^{iq_0(-\hat{\mathbf{z}})\cdot z\hat{\mathbf{z}}} e^{-i\omega t} + \text{ c.c.} = (1/2)\mathbf{E}_0 e^{-q_0 z} e^{-i\omega t} + \text{ c.c.}, \tag{14}$$

where c.c. means complex conjugate and

$$\mathbf{E}_0 = E_0[(E_{0x}/|E_0|)\hat{\mathbf{x}} + (E_{0y}/|E_0|)\hat{\mathbf{y}}], \tag{15}$$

written in this way because in general E_0 is a complex amplitude. However, we will take it to be real, so that other phases are measured relative to the incident wave, which, physically, is no loss of generality. The complex conjugate ensures the reality of the incident field. However it is easier to deal with complex phasor representations for the calculations, after which the actual fields can be reconstructed from equations of the form of (14). The phasor forms of all the equations can be derived from a Fourier transform, that transforms the electric field, for example, according to:

$$\mathbf{E}(t) = \int_{-\infty}^{+\infty} d\omega'\, \mathbf{E}(\omega') e^{-it}, \tag{16}$$

where

$$\mathbf{E}(\omega') = \frac{1}{2\pi} \int_{-\infty}^{+\infty} d\tau\, \mathbf{E}(\tau) e^{-i\omega' t}. \tag{17}$$

Note that the single frequency ω in (14) is constant with respect to the ω' integral.

With the formalism in place it is now possible to express the problem in complex phasor form. Before doing so though we pause to discuss two further simplifications that will be used: (i) The spontaneous polarization P_0 will be assumed to be constant throughout the film, corresponding to the limit as δ_1 and δ_2 approach infinity in the boundary conditions, (5) and (6). The coupled equations, (8) to (10) can then be solved analytically. Insights into the overall behavior can still be achieved, despite this simplification, and the more general case when $P_0 = P_0(z)$, which implies a numerical solution, will be dealt with in future work. (ii) Only an x polarized incident field will be considered ($E_{0y} = 0$ in (15)) and the symmetry of the film's crystal structure will be assumed to be uniaxial with the axis aligned with $\mathbf{P}_0 = P_0\hat{\mathbf{x}}$. Under these circumstances $E_\alpha = Q_\alpha = 0$, $\alpha = y,\ z$, meaning that the equations that need to be solved are reduced to (8), and (10) for $\alpha = z$.

It is a simple matter to find the bulk P_0: the free energy for the bulk does not include an integral and, as is brought out by Lines and Glass (1977), for the second-order transitions that we consider here, it is,

$$F_{\text{bulk}} = \tfrac{1}{2}AP^2 + \tfrac{1}{4}BP^4. \tag{18}$$

Minimizing by setting $dF_{\text{bulk}}/dP = 0$ yields

$$P_0 = \begin{cases} |A|/B & \text{if } T < T_c, \\ 0 & \text{if } T > T_c, \end{cases} \tag{19}$$

for real P_0(the reality of P_0 is a physical requirement).

The problem can now be solved analytically. Through (11) to (13) it can be seen that, for the single frequency applied field, there will be linear terms corresponding to frequency w and, through $\mathbf{Q}^{(2)}$ in (13), there will be nonlinear terms coming from products of the field components (only those involving E_x^2 for the case we are considering), each involving a frequency 2ω—these are the SHG terms (higher order terms will not be considered). It is natural to split the problem in to two parts now: one for

the linear terms at ω, the other for the SHG terms at 2ω. Since we are primarily interested in SHG it may seem that the linear terms do not need to be considered. However, the way that the second harmonics are generated is through the nonlinear response of the polarization to the linear applied field terms. This is expressed by the constitutive relation in (11), from which it is clear that products of the linear terms express the SHG, which implies that the linear problem must be solved before the SHG terms can be calculated. This will be much more apparent in the equations below. In view of this we give the phasor form of the problem in two parts, one for the linear terms, the other for the SHG terms.

3.2 Complex Phasor Form of the Problem for the Linear Terms

For the linear terms at frequency ω, we seek the solution to the coupled differential equations, (8) and (10) with a constitutive relation given by (12) and (13), and a P_0 given by (19). This is expressed in complex phasor form by a Fourier transform given in (16) and (17).

The resulting coupled differential equations are

$$D\frac{d^2Q^\omega}{dz^2} + M(\omega)Q^\omega + E^\omega = 0, \tag{20}$$

$$\frac{d^2E^\omega}{dz^2} + \frac{\omega^2\epsilon_\infty}{c^2}E^\omega + \frac{\omega^2}{c^2\epsilon_0 c^2}Q^\omega = 0, \tag{21}$$

for $0 \geqslant z \geqslant -L$, where the frequency dependence has been explicitly denoted for Q and E, and this also serves to denote that they are complex phasors rather than real quantities. Furthermore,

$$M(\omega) = m\omega^2 + i\omega\gamma - 2BP_0^2. \tag{22}$$

Taking the ansatz e^{iqz} for the form of the $Q^\omega$and E^ωsolutions, non trivial solutions (which are the physically meaningful ones) are obtained providing that the determinant of the coefficient matrix—generated by substituting the ansatz into (20) and (21)—satisfies

$$\begin{vmatrix} 1 & -Dq^2 + M(\omega) \\ -q^2 + \dfrac{\omega^2\epsilon_\infty}{c^2} & \dfrac{\omega^2}{\epsilon_0 c^2} = 0 \end{vmatrix} = 0. \tag{23}$$

This leads to a quadratic equation in q^2 whose solution is

$$(q_j^\omega)^2 = \frac{g_1(\omega)(-1)^{j+1}\sqrt{g_2(\omega)}}{2D}, \quad j = 1,\, 2, \tag{24}$$

where

$$g_1(\omega) = \frac{D\omega^2\epsilon_\infty}{c^2} + M(\omega), \tag{25}$$

$$g_2(\omega) = g_{1l}^2(\omega) - \frac{4D\omega^2}{\epsilon_0 c^2}\left[\epsilon_\infty\epsilon_0 M(\omega) - 1\right], \tag{26}$$

and the ω dependence of the q solutions has been made explicit with the superscript. The general solution of the coupled equations (20) and (21) for the electric field is therefore,

$$\begin{aligned} E^\omega(z) &= a_1E_0e^{-iq_1^\omega z}a_2E_0e^{iq_1^\omega z} \\ &\quad + a_3e^{iq_2^\omega z} + a_4e^{-iq_2^\omega z} \end{aligned} \tag{27}$$

$$= E_0\sum_{j=1}^{4} a_j e^{(-1)^j}q_{n_j}^\omega z, \tag{28}$$

where $n_j = \lceil j/2 \rceil$. It is convenient to include the incident amplitude E_0 as a factor expressing the constants as this will cancel when the boundary conditions are applied so that the a_1 to a_4 amplitudes are the wave amplitudes of these four waves in the film relative to the incident amplitude. The first term is a transmitted wave traveling through the film towards the metal boundary (in the direction of $-z$ in our coordinate system), the second is the wave reflected from the metal boundary and traveling back towards the top of the film corresponding to the wave vectors $-q_1^\omega$ and q_1^ω, respectively. Similar pattern follows for the last two terms in (28) for the $\pm q_2^\omega$ modes. It is interesting to note that the presence of both $\pm q_1^\omega$ modes and $\pm q_2^\omega$ is a direct result of the D term in the free energy that is introduced to account for variations in the polarization. In this sense are calculation, despite using a constant P_0 value, is still incorporating the effects of varying polarization (the full effects, as discussed above, involve numerical calculations which will not be done in this paper). If there was no D term then only the $\pm q_1^\omega$ modes would be present and the character of the solution would be different.

Above the film, alongside the incident wave there is a reflected wave. Thus we have

$$E_{\mathrm{I}}^\omega(z) = E_0e^{-iq_0z} + rE_0e^{iq_0z}, \quad z > 0 \tag{29}$$

where r is the linear reflection coefficient (there will also be a wave from SHG which is considered in the next section).

To complete the solution of the linear problem it remains to calculate the a_j and r amplitudes (5 in total) by applying boundary conditions. The boundary conditions are the usual electromagnetic boundary conditions of continuity of the electric and magnetic fields, and here, we will express the continuity of the magnetic field as the continuity of $d\mathbf{E}/dz$; this follows from the electromagnetic induction Maxwell equation, $\boldsymbol{\nabla}\times\mathbf{E} = -\partial\mathbf{B}/\partial t$ (since the film is nonmagnetic $\mathbf{B} = \mu_0\mathbf{H}$ not only above the film but also in the film). The boundary conditions on $\mathbf{P}$ in (5) and (6) will also be used in the limiting case of infinite extrapolation lengths.

In view of the forgoing the required boundary conditions are:

$$E_{\mathrm{I}}^\omega(0) = E^\omega(0), \;\left.\frac{dE_{\mathrm{I}}^\omega}{dz}\right|_{z=0} = \left.\frac{dE^\omega}{dz}\right|_{z=0}, \;\left.\frac{dQ^\omega}{dz}\right|_{z=0} = 0, \tag{30}$$

for the top surface, and

$$E^\omega(-L) = 0, \;\left.\frac{dQ^\omega}{dz}\right|_{z=-L} = 0, \tag{31}$$

for the film-metal interface at the bottom. Note that the electric field boundary condition at the bottom implies that the metal conductivity is infinite so that no electric field penetrates the metal. This is a common approximation for metal boundaries and should be sufficient for our purposes since the conductivity of the ferroelectric film is much smaller than for the metal (see Webb (2006) for more on this). Also the continuity of the magnetic field is not used at the bottom; it is not required because, with 5 unknowns, 5 boundary conditions are sufficient to find them.

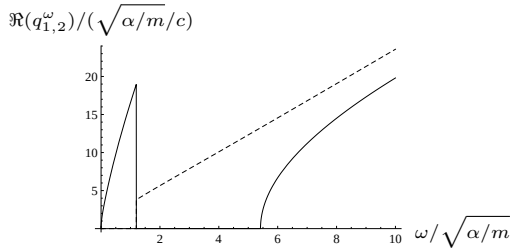

Fig. 1. Dimensionless plot of $\Re(q_1^\omega)$ and $\Re(q_2^\omega)$ (dotted line) versus frequency for $a = 6.8 \times 10^5$ V K^{-1}A^{-1}s^{-1}, $D = 2.7 \times 10^{-21}$ A Kg^{-1}m^{-1}, $m = 6.4 \times 10^{-21}$ kg m^{3}A^{-1}s^{-2}, $L = 40$ nm, $T/T_c = 0.5$, $\gamma = 1.3 \times 10^{-9}$ A^{-1}V^{-1}m^{-3}, and $\epsilon_\infty = 3.0$. These values are for $BaTiO_4$, and follow Chew et al. (2001).

Applying the boundary conditions leads to a set of simultaneous equations, the solution of which yields expressions for r and the a_j in terms of the other parameters, and hence solves the linear problem. These equations may be expressed in matrix form as

$$\mathsf{M}(\omega)\mathsf{a}_{\rm lin} = \mathsf{b}_{\rm lin}, \tag{32}$$

where

$$\mathsf{M}(\omega) = \begin{pmatrix} 1 & 1 & 1 & 1 & -1 \\ q_1^\omega & -q_1^\omega & q_2^\omega & -q_2^\omega & q_0 \\ \kappa_1^\omega & \kappa_2^\omega & \kappa_3^\omega & \kappa_4^\omega & 0 \\ \Delta_1^\omega & \Delta_2^\omega & \Delta_3^\omega & \Delta_4^\omega & 0 \\ \kappa_1^\omega\Delta_1^\omega & \kappa_2^\omega\Delta_2^\omega & \kappa_3^\omega\Delta_3^\omega & \kappa_4^\omega\Delta_4^\omega & 0 \end{pmatrix}, \tag{33}$$

$$\mathsf{a}_{\rm lin} = (a_1,\, a_2,\, a_3,\, a_4,\, r)^{\mathsf{T}}, \tag{34}$$

$$\mathsf{b}_{\rm lin} = (1,\, q_0,\, 0,\, 0,\, r)^{\mathsf{T}}, \tag{35}$$

and we define

$$\kappa_j^\omega = (-1)^j q_{n_j}^\omega \left[(q_{n_j}^\omega)^2 - \epsilon_\infty q_0^2\right],\ \Delta_j^\omega = e^{(-1)^{j+1} i q_{n_j} L}. \tag{36}$$

The resulting symbolic solution is rather complicated and will not be given here explicitly. It is easily obtained, however, with a computer algebra program such as Maxima or Mathematica. A more efficient approach for numerical plots is to compute numerical values of all known quantities before solving the matrix equation, which is then reduced to a problem involving the 5 unknowns multiplied by numerical constants.

The real parts of the dispersion relations in (24) are plotted in Fig. 1. for the q_1^ω and q_2^ω modes. The q_1^ω mode is the usual mode found in dielectrics and the frequency region, known as the reststrahl region, in which it is zero is where there are no propagating waves for that mode. However, it is clear from the plot that the real part of q_2^ω mode is not zero in this region and so there will be propagation leading to a different reflection coefficient than what would be observed. This is due to the effect of the D term.

In Fig. 2 the magnitude of reflection the coefficient r—available from the solution to the linear problem—is plotted against frequency. With no D term the reflection coefficient would be 1 in the reststrahl region. It is clear from the plot that there is structure in this region that is caused by the q_2^ω mode. So reflection measurements are a way of investigating the varying polarization modeled through the D term. The plot is for a film thickness of 40 nm. So our model predicts that these effects will be significant for nanoscale films. It is also expected that structure in this

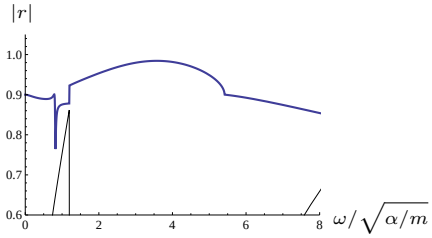

Fig. 2. Magnitude of linear reflection coefficient r versus dimensionless frequency. The lower curve is a scaled down plot of the dispersion curve for q_1^ω showing the reststrahl region. Parameter values as in Fig. 1.

region will be found for the SHG reflection, the calculation of which which we now turn to.

3.3 Complex Phasor Form of the Problem for the Nonlinear SHG Terms

The SHG terms come from the second order nonlinear terms at frequency 2ω and the coupled differential equations that need to be solved for these terms are

$$D\frac{d^2Q^{2\omega}}{dz^2} + M(2\omega)Q^{2\omega} + E^{2\omega} = 3BP_0^2[Q^\omega]^2, \tag{37}$$

$$\frac{d^2E^{2\omega}}{dz^2} + \frac{2\omega^2\epsilon_\infty}{c^2}E^{2\omega} + \frac{(2\omega)^2}{c^2\epsilon_0 c^2}Q^{2\omega} = 0, \tag{38}$$

$$\text{for } 0 \geqslant z \geqslant -L.$$

It can be seen from this that there will be a homogeneous solution analogous to the linear solution but now at frequency 2ω and in addition, due to the term involving $[Q^\omega]^2$ in (37), there will be particular solutions. $[Q^\omega]^2$ can be found from the solution to the linear problem for E^ω substituted into (21), and thus the particular solutions to (37) and (38) can be determined. In this way the general solution can be shown to be given by

$$E_0^2\Lambda\sum_{j=1}^{4}\phi_j e^{(-1)^j i q_{n_j}^{2\omega} z} + E_0^2\sum_{j=1}^{4}\sum_{k=1}^{4} W_{jk}e^{iB_{jk}z}, \tag{39}$$

together with,

$$W_{jk} = \frac{12BP_0^2A_{jk}}{\epsilon_0\left[4q_0^2\epsilon_\infty - B_{jk}^2\right]\left[DB_{jk}^2 - M(2\omega)\right]}, \tag{40}$$

$$A_{jk} = S_{n_j}S_{n_k}a_j a_k, \tag{41}$$

$$s_j = (q_j^\omega)^2 - \epsilon_\infty\omega/c^2, \tag{42}$$

$$B_{jk} = (-1)^j q_{n_j}^\omega + (-1)^k q_{n_k}^\omega. \tag{43}$$

It is convenient to include the factor E_0^2 in (39) since it will cancel out later when the boundary conditions are applied. The factor Λ has been included to make the ϕ_j amplitudes dimensionless so that they are on the same footing as the a_j amplitudes in the linear problem.

Due to the SHG terms in the film there will also be an SHG field transmitted from the film to the air above, but since this ultimately exists because of the incident field the SHG wave above the film is a reflected wave caused by the incident field. It is expressed by

$$E_{\rm I}^{2\omega}(z) = E_0^2\Lambda\rho e^{2iq_0 z}, \quad z > 0, \tag{44}$$

where ρ is the SHG reflection coefficient.

Again there are 5 unknowns: ρ and the ϕ_j, which are also found by applying the boundary conditions. The particular solutions make the problem more complex algebraically,

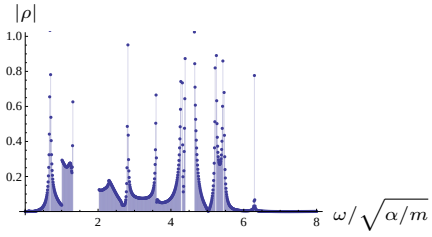

Fig. 3. SHG reflection coefficient ρ versus dimensionless frequency. Parameter values are as in Fig. 1.

but in principle the solution method is the same as for the linear case. Applying the conditions in (30) and (31) leads to five simultaneous equations that can be expressed as

$$\mathsf{M}(2\omega)\mathsf{a}_{\mathrm{SHG}} = \mathsf{b}_{\mathrm{SHG}}, \tag{45}$$

where

$$\mathsf{a}_{\mathrm{SHG}} = (\phi_1,\ \phi_2,\ \phi_3,\ \phi_4,\ \rho)^{\mathsf{T}}, \tag{46}$$

$$\mathsf{b}_{\mathrm{SHG}} = (\mathcal{P}_1,\ \mathcal{P}_2,\ \mathcal{P}_3,\ \mathcal{P}_4,\ \mathcal{P}_5)^{\mathsf{T}}, \tag{47}$$

with

$$\left.\begin{array}{c} \mathcal{P}_1 = -(1/\Lambda)\sum_{jk} W_{jk},\ \mathcal{P}_2 = (1/\Lambda)\sum_{jk} W_{jk}B_{jk}, \\ \mathcal{P}_3 = (1/\Lambda)\sum_{jk} W_{jk}O_{jk},\ \mathcal{P}_4 = -(1/\Lambda)\sum_{jk} W_{jk}\delta_{jk}, \\ \mathcal{P}_5 = (1/\Lambda)\sum_{jk} W_{jk}O_{jk}\delta_{jk}, \end{array}\right\} \tag{48}$$

and

$$O_{jk} = B_{jk}\big(4\epsilon_\infty q_0^2 - B_{jk}^2\big), \quad \delta_{jk} = e^{-iB_{jk}L}. \tag{49}$$

Now the unknowns for the SHG problem can be found by solving (42), in a similar way to what was done for the linear problem, and from this the SHG reflection coefficient ρ can be found.

A plot of $|\rho|$ versus frequency is given in Fig. 3. A dramatic structure is evident and, as with the linear reflection, is also present in the reststrahl region. So SHG reflection measurements are expected to be a sensitive probe of size effects in nanoscale ferroelectric thin films according to the model presented in this paper.

The numerical values calculated for the SHG reflection coefficient are much smaller than for the linear one. This is to be expected since SHG is a second-order nonlinear effect. This numerical result is consistent with that found by Murgan et al. (2004), but their work did not include the mode due to the D term. Also the general features of the SHG reflection coefficient are similar to a brief SHG study that was done by Stamps and Tilley (1999) for a free standing film. However the effect of the metal substrate considered here has made the SHG reflection features more pronounced.

It is also of interest to compare the numerical values here with experimental studies. Many SHG reflection experimental studies have covered optical frequencies higher than the far-infrared frequencies that are relevant to the work in this paper. It is hoped that our work will stimulate more experimental work in the far-infrared region. Detailed numerical work that is now in progress can then be compared with such experiments.

REFERENCES

O. Auciello, J. F.Scott, and R. Ramesh. The physics of ferroelectric memories. *Phys. Today*, 51:22, 1998.

Y. Barad, J. Lettieri, C. D. Theis, D. G. Schlom, V. Gopalan, J. C. Jiang, and X. Q. Pan. Probing domain microstructure in ferroelectric $Bi_4Ti_3O_{12}$ thin films by optical second harmonic generation. *Appl. Phys. Lett.*, 89:1387, 2001.

D. J. Bottomley, G. Lupke, J. G. Mihaychuk, and H. M. van Driel. Determination of the crystallographic orientation of cubic media to high resolution using optical harmonic generation. *Appl. Phys. Lett.*, 89:1387, 2001.

P. N. Butcher and D. Cotter. *The Elements of Nonlinear Optics*. Cambridge University Press, Cambridge, UK, 1990.

K. H. Chew, J. Osman, R. L. Stamps, D. R. Tilley, and J. F. Webb. Theory of far infrared spectroscopy for ferroelectric size effects. *Integrated Ferroelectrics*, 23: 161, 1999.

K. H. Chew, L. H. Ong, J. Osman, and D. R. Tilley. Theory of far-infrared reflection and transmission by ferroelectric thin films. *J. Opt. Soc. Am. B*, 18:1512, 2001.

V. Gopalan and R. Raj. Domain structure and phase transitions in $KNbO_3$ thin films observed by *in-situ* second harmonic generation. *Appl. Phys. Lett.*, 68:1323, 1996.

M. E. Lines and A. M. Glass. *Principles and Applications of Ferroelectrics and Related Materials*. Clarendon, Oxford, UK, 1977.

D. L. Mills. *Nonlinear Optics*. Springer-Verlag, Berlin, 1991.

E. D. Mishina, N. E. Sherstyuk, D. Barsky, A. S. Sigov, Yu. I. Golovko, V. M. Mukhorotov, M. De Santo, and Th. Rasing. Domain orientation in ultrathin $(BaSr)TiO_3$ films measured by optical second harmonic generation. *J. Appl. Phys*, 93:6216, 2003.

R. Murgan, F. Razak, D. R. Tilley, T. Y. Tan, J. Osman, and M. N. A. Halif. Second harmonic generation from a ferroelectric film. *Comp. Mat. Sci*, 30:468, 2004.

L. H. Ong, J. Osman, and D. R. Tilley. Landau theory of second-order phase transitions in ferroelectric films. *Phys. Rev. B*, 63:144109, 2001.

J. F. Scott. *Ferroelectric Memories*. Springer, Berlin, 1992.

J. F. Scott. The physics of ferroelectric ceramic thin films for memory applications. *Ferroelectr. Rev.*, 1:1, 1998.

R. L. Stamps and D. R. Tilley. Possible far infrared probes of ferroelectric size effects. *Ferroelectrics*, 230:221, 1999.

B. A. Strukov and A. P. Lenanyuk. *Ferroelectric Phenomena in Crystals*. Springer, Berlin, 1998.

A. K. Tagantsev, G. Gerra, and N. Setter. Short-range and long-ragne contributions to the size effect in metal-ferroelectric hetrostructures. *Phys. Rev. B*, 77:174111, 2008.

E. K. Tan, J. Osman, and D. R. Tilley. First-order phase transitions in ferroelectric films. *Solid State Commun.*, 116:61, 2000.

D. R. Tilley. Phase transitions in thin films. In N. Setter and E. L. Colla, editors, *Ferroelectric Ceramics*, page 163. Birkhauser Verlag, Basel, 1993.

D. R. Tilley and B. Zeks. Landau theory of phase transitions in thick films. *Solid State Commun.*, 49:823, 1984.

J. F. Webb. Theory of size effects in ferroelectric ceramic thin films on metal substrates. *J. Electroceram.*, 16:463, 2006.